

Electron spin resonance investigation of F_6^{5-} centres in LiF:Co and LiF:Ni

This article has been downloaded from IOPscience. Please scroll down to see the full text article.

1991 J. Phys.: Condens. Matter 3 83

(<http://iopscience.iop.org/0953-8984/3/1/006>)

View [the table of contents for this issue](#), or go to the [journal homepage](#) for more

Download details:

IP Address: 171.66.16.151

The article was downloaded on 11/05/2010 at 07:03

Please note that [terms and conditions apply](#).

Electron spin resonance investigation of F_6^{5-} centres in LiF:Co and LiF:Ni

G M Nurullin, L N Galygo, A V Egranov and A I Nepomnyachikh

Institute of Geochemistry, Academy of Sciences of the USSR, Favorskii Street 1a, 664033 Irkutsk, USSR

Received 21 February 1990, in final form 16 July 1990

Abstract. Two types of tetragonal centre have been discovered in LiF:Co. One centre produced by x-irradiation at 77 K is converted by heating into another centre. The latter is stable up to 180 °C. A large splitting with two equivalent fluorine atoms and a small splitting with four equivalent fluorine atoms are observed in both centres. HFS caused by the Co nucleus is absent. These defects are molecular ions F_6^{5-} bonded with an impurity. The broad line of Co^+ is observed too.

1. Introduction

Centres discovered after x-irradiation in LiF:Co resemble defects VI and VII observed by Hayes and Wilkens [1] in x-irradiated LiF:Ni. These centres were interpreted as different states of the Jahn–Teller ion Ni^+ occupying the cation site. The analogue of centre VII in NaF:Ni was observed too, namely the 'F' centre. Comparing the VII and F centres, Hayes and Wilkens concluded that HFS is caused by fluorine nuclei only. The absence of Ni nucleus splitting is explained by the small amount of ^{61}Ni (1.19%), but the absence of ^{59}Co (100%) nucleus splitting in our experiments suggest that the impurity ion does not occupy the central position in the defects.

Kuwabara [2] produced the centres $Ni^+ I$ and $Ni^+ II$ in NaCl by x-irradiation. These centres are similar to centres VI and VII in LiF:Ni. Bacquet *et al* [3] reported defects in x-irradiated LiF:Ba. These defects are probably related to the centres VI and VII in LiF:Ni, but in LiF:Ba a paramagnetic particle interacts with six equivalent fluorine nuclei.

Interaction with the nuclei of Li and Na does not appear in all the cases mentioned above; this is very typical of hole centres.

The impurity position in LiF:Co and LiF:Ni before irradiation is not clear. Besides the usual models, Musa [4] proposed a model of interstitial entry of Co^{2+} into the alkali halide matrix. Also Ikrami *et al* [5], in determining the chemical composition of LiF:Co, LiF:Ni, NaF:Co and NaF:Ni, established the general structural formula for these crystals:



where Me^+ is an alkaline metal and Me^{2+} is a transition metal, $0.0005 \leq x \leq 0.015$. Our results confirm this formula and Musa's hypothesis indirectly.

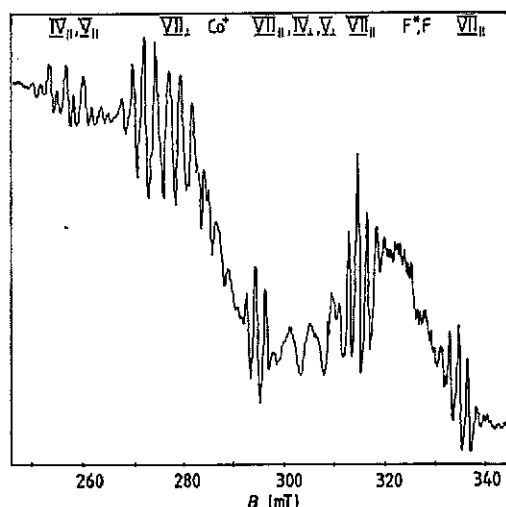


Figure 1. ESR spectrum of the LiF:Co after x-irradiation at RT (recording temperature, 77 K; $B \parallel \langle 100 \rangle$; $\nu = 9.0970$ GHz). The centres IV and V (see [1]) are not discussed in this paper.

This paper basically concerns centres VI and VII and the Co^+ line; other centres are discussed briefly.

2. Experimental details

Crystals of LiF:Co and LiF:Ni were grown from the melt by the Stockbarger method in a fluorine atmosphere. The impurity concentrations determined by spectral analysis were 0.25 wt% Co and 0.55 wt% Ni. The crystals were x-irradiated for 1 h at room temperature (RT) with the tube operating at 40 kV and 50 mA. All centres were created in this way except centre VI. Centre VI was created by x-irradiation at liquid-nitrogen temperature (LNT). ESR spectra were recorded at LNT because centres VI do not exist and centres VII are not visible at RT. Apparatus for recording at temperatures below LNT was not available.

3. Results

3.1. Broad lines

3.1.1. LiF:Co. Before irradiation, paramagnetic centres were not observed. After irradiation a broad anisotropic line of abnormal form appears. This line has a steep slope towards the high magnetic field and is destroyed between 50 and 130 °C. In figures 1 and 2 and table 1 the line is marked as Co^+ .

Another broad line is also observed after irradiation. The line has a g -factor approximately the same as the F centre and is marked as F^* in figure 1; it is not discussed in this paper.

Table 1. Parameters of the broad line spectra. ΔB are the linewidths between extremes of the first derivative. The errors were ± 1 mT and ± 0.007 for ΔB and the g -factor, respectively.

	KCl:Co ⁺ [6]	NaCl:Co ⁺ [7]	LiF:Co ⁺			LiF:Ni ²⁺		
			$\langle 100 \rangle$	$\langle 110 \rangle$	$\langle 111 \rangle$	$\langle 100 \rangle$	$\langle 110 \rangle$	$\langle 111 \rangle$
g , before irradiation	2.14					2.05	2.30	2.32
g , after irradiation		2.049(2)	2.12	2.25	2.22	2.13	2.24	2.30
ΔB (mT) before irradiation	10					97	56	46
ΔB (mT) after irradiation		6.2(3)	28	35	35	63	35	27

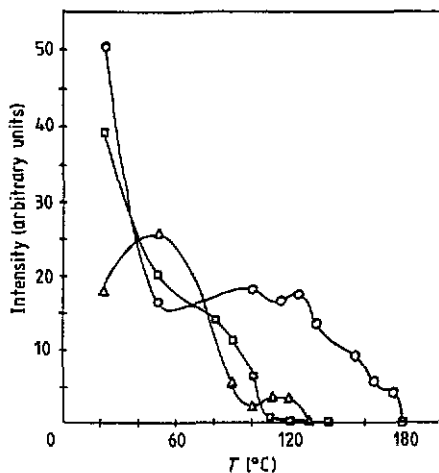


Figure 2. The annealing curves of the line intensities. The crystals were kept for 10 min at each temperature; \circ , centres VII in $LiF:Co$; \square , centres VII in $LiF:Ni$; \triangle , line Co^+ in $LiF:Co$.

3.1.2. *LiF:Ni.* Before irradiation a well known broad anisotropic line is observed [1]. It is clear that the line consists of several components, which greatly overlap (see table 1).

3.2. Centres VI in $LiF:Co$

Centres very similar to centres VI in $LiF:Ni$ are observed after irradiation at LNT. We are convinced that it is possible to create centres VII via centres VI by heating a crystal to RT. The exact temperature of the conversion of centres VI to centres VII was not established.

3.3. Centres VII in $LiF:Co$ and $LiF:Ni$

These centres are observed in both crystals after irradiation at RT. We shall describe these centres for both crystals simultaneously because of the striking resemblance of the spectra.

3.3.1. Number and intensity of lines. For $B\|\langle 100 \rangle$ (figure 1) a triplet in a high field with an intensity distribution of 1:2:1 is observed. Each triplet component is split into a quintet with a distribution of 1:4:6:4:1. A nonet with a distribution of 1:4:8:12:14:12:8:4:1 is observed in a low field. The nonet is more intensive than the triplet, by a factor of approximately 2.

For $B\|\langle 110 \rangle$, the spectrum is different from that for $B\|\langle 100 \rangle$.

- (i) The triplet is more intensive than the nonet, by a factor of approximately 2.
- (ii) The three central components of the quintets are broadened.
- (iii) The nonet components are split into doublets, whose components are spaced by 0.84 mT and 0.81 mT in LiF:Co and LiF:Ni, respectively.

For $B\|\langle 111 \rangle$, a triplet with a distribution of 1:2:1 is observed. Each triplet component is split into an octet. It is difficult to estimate the intensity distribution within the octet because of overlapping. Six central octet lines are grouped into doublets, whose components are spaced by 1.15 mT and 0.98 mT in LiF:Co and LiF:Ni, respectively.

3.3.2. *g*-factor. Data on the *g*-factor are presented in figures 3(a) and 3(b) and table 2, where θ is the angle between the external magnetic field B and $\langle 100 \rangle$. When there are two values of the *g*-factor, this corresponds to the doublet splitting in the spectra for $B\|\langle 100 \rangle$ and $B\|\langle 111 \rangle$.

3.3.3. HFS constants. Data on the A -tensor are presented in figures 3(c) and 3(d) and table 3. A^I and A^{II} are splittings due to nuclei types I and II, respectively; α is the angle between the bond line of the type I nucleus and B (figure 4).

3.3.4. Thermal stability. Figure 2 gives the annealing curves. Defects are destroyed at 180 °C and 140 °C in LiF:Co and LiF:Ni, respectively.

4. Discussion

4.1. Broad lines

There are two most likely configurations according to formula (1).

- (i) The interstitial impurity ion Me^{2+} is compensated by the interstitial ion F^- and cation vacancy (see, e.g., figure 4(a)).
- (ii) Me^{2+} occupying the cation site is compensated by the interstitial ion F^- .

4.1.1. LiF:Ni. Probably the two configurations mentioned above cause the broad line.

4.1.2. LiF:Co. The broad line marked as Co^+ may be ascribed to Co^+ aggregates according to its *g*-factor (see table 1). The steep slope towards the high field is interpreted as due to deviation from octahedral symmetry [8]. This deviation is probably due to interaction between Co^+ and F_0^- ion (see figures 4(b) and 4(c)). It is likely that the

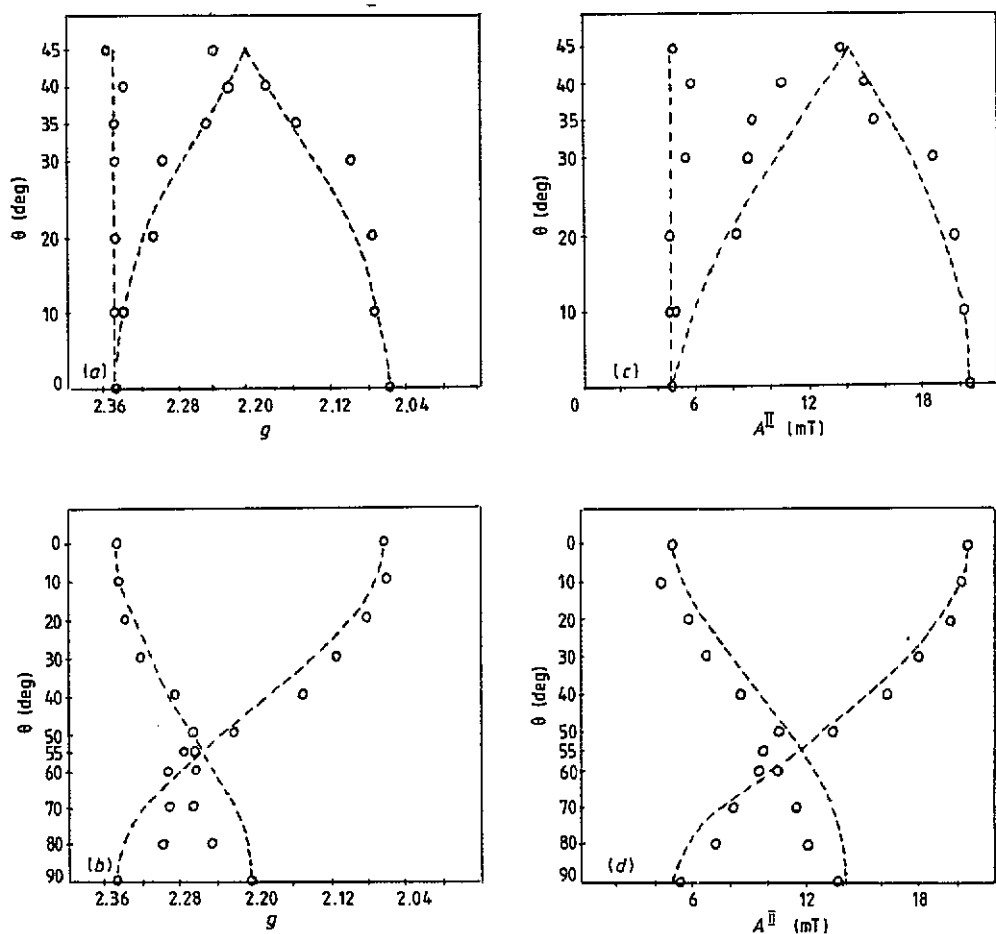


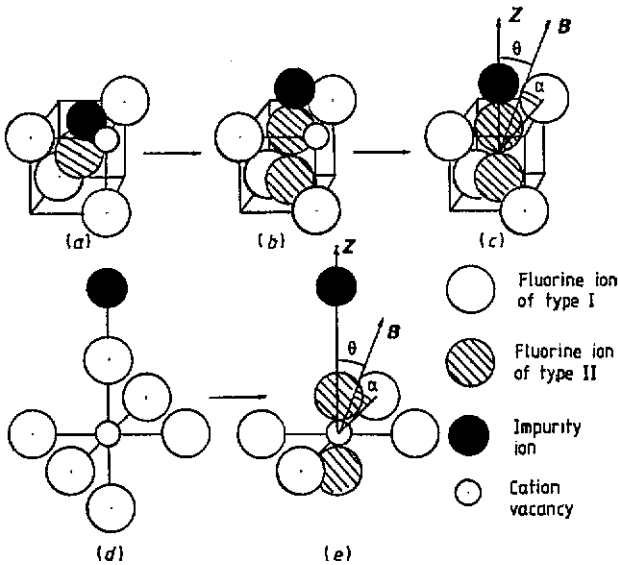
Figure 3. (a), (b) Angular dependences $g = g(\theta)$ and (c), (d) $A^{\text{II}} = A^{\text{II}}(\theta)$ for the centre VII in LiF:Co for the rotations around (a), (c) $\langle 100 \rangle$ and (b), (d) $\langle 110 \rangle$: ---, theoretical values.

Table 2. Parameters of the centre VII spectra. ΔB are the linewidths between extremes of the first derivative. The errors were ± 0.1 mT and ± 0.0007 for ΔB and the g -factor, respectively. The values calculated according to equation (3) are in parentheses.

	$\langle 100 \rangle$		$\langle 110 \rangle$		$\langle 111 \rangle$ g	ΔB		
	g_{\parallel}	g_{\perp}	g_{\perp}	$g_{\theta=45^\circ}$		$\langle 100 \rangle$	$\langle 110 \rangle$	$\langle 111 \rangle$
LiF:Co	2.0665	2.3513	2.3516 (2.3513)	2.2112 (2.2135)	2.2707 2.2795 (2.2604)	0.86	1.10	0.56
LiF:Ni	2.0681	2.3491	2.3557 2.3629 (2.3491)	2.2212 (2.2131)	2.2520 2.2596 (2.2593)	0.99	1.25	0.63

Table 3. HFS constants of the centre VII. The errors were ± 3 MHz.

	$\langle 100 \rangle$			$\langle 111 \rangle$	
	$ A_{\parallel}^{\text{I}} $ (MHz)	$ A_{\perp}^{\text{II}} $ (MHz)	$ A_{\parallel} $ (MHz)	$\langle 110 \rangle$ $ A_{\theta=45^\circ}^{\text{II}} $	$ A_{\alpha=90^\circ}^{\text{II}} $ (MHz)
LiF:Co	590.3	160.6	51.5	418.7	301.5
LiF:Ni	596.0	161.1	53.8	393.0	342.2

**Figure 4.** Models of defects in LiF:Co and LiF:Ni; (a), (d) models of crystals before irradiation; (b) HI-type model of the centres VI; (c) HI-type model of the centre VII; (e) V-type model of the centre VII. Li⁺ ions are not shown.

deviation and $S \geq 1$ lead to the abnormal line width, because of the inhomogeneous zero-field splitting parameter D [8].

4.2. Centres VI and VII in LiF:Co and LiF:Ni

In considering centre VII we shall neglect the influence of cations and impurities using the spin Hamiltonian given by

$$\frac{\mathcal{H}}{g_0 \mu_B} = \frac{1}{g_0} \mathbf{B} \cdot \mathbf{gS} + \sum_{i=1}^6 \mathbf{S} \cdot \mathbf{A} \mathbf{I}_i \quad (2)$$

where the sum corresponds to the six fluorine nuclei of types I and II.

The theoretical curves corresponding to the axial symmetry relative to $\langle 100 \rangle$ in figure 3 were calculated using the expressions

$$g^2(\theta) = g_{\parallel}^2 \cos^2 \theta + g_{\perp}^2 \sin^2 \theta \quad (3)$$

$$(A^{\parallel})^2(\theta)g^2(\theta) = (A_{\parallel}^{\parallel})^2g_{\parallel}^2 \cos^2 \theta + (A_{\perp}^{\parallel})^2g_{\perp}^2 \sin^2 \theta \quad (4)$$

where g_{\parallel} , g_{\perp} , $A_{\parallel}^{\parallel}$ and A_{\perp}^{\parallel} were taken from the spectrum for $B_{\parallel}\langle 100 \rangle$. It is clear that the principal axes of the \mathbf{g} - and \mathbf{A} -tensors are $\langle 100 \rangle$, $\langle 010 \rangle$ and $\langle 001 \rangle$ (see figure 3).

4.2.1. Models. There are two decisive arguments in favour of hole models for centres VI and VII: the absence of HFS due to the Co nucleus and the fact that the spectra have almost the same parameters for LiF:Co and LiF:Ni. Models of hole centres are presented in figures 4(b), 4(c) and 4(e). We shall call the models in figures 4(b) and 4(c) the HI-type models, and that in figure 4(e) the V-type model. The letter I signifies the existence of I centres in a non-irradiated crystal, and the letters H and V are connected with the formation processes (see below). The fluorine ions are divided into two groups according to the experimental data: a large splitting with two nuclei of type II and a small splitting with nuclei of type I are observed. We are dealing with the ion F_2^{2-} in both model types. Following the experimental results the z axis is parallel to $\langle 100 \rangle$. According to the presented models a triplet and a nonet in the $B_{\parallel}\langle 100 \rangle$ spectrum correspond to the parallel and perpendicular spectra, respectively.

The intensity ratios of the perpendicular to the parallel spectra in all directions of \mathbf{B} , and the angular dependences of the \mathbf{g} - and \mathbf{A} -tensors clearly demonstrate the tetragonal symmetry of centre VII. These experimental data correspond to both model types.

Analysis of HFS caused by nuclei of type I leads to the following.

(i) For $B_{\perp}\langle 100 \rangle$, the perpendicular spectrum according to HI model is explained by assuming the causal equation $A_{\perp}^{\parallel} = 2A_{\alpha=54.74}^{\parallel}$. The V model requires stronger terms, namely the causal equations $A_{\perp}^{\parallel} = 2A_{\alpha=0^\circ}^{\parallel}$ and $A_{\alpha=0^\circ}^{\parallel} = A_{\alpha=90^\circ}^{\parallel}$; the latter is unlikely.

(ii) For $B_{\parallel}\langle 110 \rangle$, the doublet splitting of the perpendicular spectrum nonet may be interpreted as $A_{\alpha=35.26}^{\parallel} \neq A_{\alpha=90^\circ}^{\parallel}$ according to the HI model. The V model does not explain the splitting.

(iii) For $B_{\parallel}\langle 111 \rangle$, the HI model explains octets observed in the experiment and it is easy to explain the doublet grouping by supposing that the splitting on the three equivalent nuclei is less than on the fourth nucleus: $A_{\alpha=0}^{\parallel} \approx 1.33A_{\alpha=90^\circ}^{\parallel}$. The V model has to give quintets instead of octets.

Thus the HI model corresponds to HFS better than the V model does.

It is possible to suppose that the hole density located on nuclei of type II in centres VI and VII is smaller than that located on the components of F_2^- in the H centre ($A_{\parallel} = 2818.1$ MHz [9]) and in V_K centre ($A_{\parallel} = 2486.8$ MHz [10]). Probably, the hole density located on the nuclei of type I is larger than that located on the nuclei which do not belong to F_2^- in the H and V_K centres.

It is reasonable to suppose that the $(F_2^-)^{\parallel}$ ion is situated inside the tetrahedron formed by nuclei of type I, which are slightly shifted from the sites of the lattice along approximately $\langle 111 \rangle$ from the centre of the tetrahedron.

The fact that the destruction temperatures for the centre VII and the line Co^+ in LiF:Co are approximately the same arise because the centre VII is closely bonded to an impure ion Me^+ . It is likely that the abnormal thermal stability for the hole centres of VII is due to its electroneutrality.

4.2.2. *Formation processes.* In the HI model (figures 4(a)–(c)), the molecular ion $(F_2^-)^{II}$ is formed as a result of irradiation at LNT, probably according to the H-centre scheme. At the same time Me^{2+} is reduced to Me^+ . In this way the centre VI is formed. Centres VI and VII have very similar ESR parameters. Centre VI probably has a total negative electrical charge of one unit. At about 240 K, centre VI is converted to centre VII. Perhaps this occurs because the cation vacancy moves away [1].

After irradiation at RT, centre VI is not observed because the vacancy moves away immediately. In other respects the formation of centre VII at RT is the same as that at LNT.

In the V model (figures 4(d) and 4(e)), it is difficult to imagine the formation of centre VI. The molecular ion $(F_2^-)^{II}$ may be formed according to the V_K -centre scheme after irradiation at both LNT and RT.

The formation processes based on the HI model look more likely.

4.2.3. *Conclusions for centres VI and VII.* These are as follows.

(i) These centres have a hole nature and are molecular F_6^{5-} ions bonded with an impurity.

(ii) In the main, the hole density is located on the two equivalent fluorine ions; the remaining part of the hole density is located on the four equivalent ions forming the tetrahedron.

(iii) The centres have tetragonal symmetry.

(iv) The impurity ion is probably monovalent.

(v) It is likely that the centre VI has one unit negative charge and the centre VII is electroneutral.

References

- [1] Hayes W and Wilkens J 1964 *Proc. R. Soc. A* **281** 340
- [2] Kuwabara G 1971 *J. Phys. Soc. Japan* **31** 1074
- [3] Bacquet G, Dugas J and Gautier P 1967–8 *J. Physique Suppl.* **28** 100
- [4] Musa M 1966 *Phys. Status Solidi* **16** 771
- [5] Ikrami J, Sidorow V, Olchovaya L, Luginina A and Ikrami M 1989 *Proc. Vacuum Ultra-Violet Conference (Irkutsk 1989)* vol 1, p 110
- [6] Mehendry P C and Narendra K 1975 *Phys. Status Solidi* **b 68** K129
- [7] Jain S C and Krishan L 1970 *Cryst. Lattice Defects* **1** 165
- [8] Abragam A and Bleaney B 1970 *Electron Paramagnetic Resonance of Transition Ions* vol 1 (Oxford: Clarendon) ch 7, section 15
- [9] Hou Chu Y and Mieher R L 1969 *Phys. Rev.* **188** 1311
- [10] Woodruff T and Kanzig W 1958 *J. Phys. Chem. Solids* **5** 268